

# Simulation of Model Predictive Control – Space Vector Modulation fed PMSM drive

Megha Mohan

Dept. of Electrical & Electronics  
Rajagiri School of Engineering & Technology  
Kochi, Kerala

Jayasri R. Nair

Dept. of Electrical & Electronics  
Rajagiri School of Engineering & Technology  
Kochi, Kerala

**Abstract**—To achieve high dynamic torque control for Permanent Magnet Synchronous Motor (PMSM) drives, a Model Predictive Control (MPC) scheme is introduced in this paper. The basic idea of MPC is to predict the future behavior of control variables in the time domain based on the model of the control system and choose the control action according to an optimization cost function. This work proposes a Model Predictive Control – Space Vector Modulation (MPC-SVM) technique for PMSM drives, combines the advantage of both SVM technique and MPC, which overcomes the problem of high ripple in the electromagnetic variables and provides a fixed switching frequency for the voltage source inverter that feeds the motor. Simulation analysis has been done to demonstrate the effectiveness of the proposed scheme.

**Keywords**— Permanent Magnet Synchronous Motor (PMSM); Model Predictive Control (MPC); Space Vector Modulation(SVM)

## I. INTRODUCTION

AC motors are dominating the drive market nowadays and have replaced the DC motor in high performance applications where variable speed and torque control is needed. Permanent Magnet Synchronous Machines are widely used in electrical drives because of their several advantages in terms of high efficiency, high power density, high torque to weight ratio and excellent dynamic performance, which makes it suitable for many industrial applications such as electric vehicles, servo control system, wind power generation etc. The high performance PMSM drives require high dynamic control strategies.

The two most popular variable speed control strategies for PMSMs are Field Oriented Control (FOC) and Direct Torque Control. The basic principle behind FOC is to decouple torque and flux which is similar to that of DC machines and thus enables an independent control of field and torque by manipulating the corresponding field oriented quantities. They are usually employed for the applications requiring high dynamic performance. But their main limitations are high sensitivity to machine parameters and large computing cost. Conventional DTC based on hysteresis comparators and switching table is a widely accepted control method. DTC selects the desired voltage vector and applies directly to the inverter fed PMSM. DTC features fast dynamic response, robustness to parameter variations and simple structure, which makes them applicable to medium and high power electric drives. The major drawbacks of DTC are large torque and flux ripples, variable switching frequency and acoustic noise. A DTC

scheme for PMSM drive was proposed in [2]. In [3], the principles of sliding mode control and SVM are combined with DTC to achieve better performance. But it reduces the simplicity of classic DTC scheme.

Due to several disadvantages of classic FOC and DTC, an alternating strategy called MPC which is one of the predictive control methods, has emerged to achieve high dynamic torque control for electric drives. MPC uses the mathematical model of the system to precalculate the systems behavior and to determine optimum values for the actuating variables from these precalculated values. The three main steps of MPC are prediction, estimation and cost function minimization. The definition of the cost function is related to the control objectives and the key technology of MPC lies in this cost function definition. All predictions are evaluated by this cost function and future control actions can be implemented by choosing the one with the minimum cost. The main advantage of MPC is the easy inclusion of constraints and nonlinearities. There are mainly two types of MPC, Finite Control Set MPC (FCS-MPC) and Continuous Control Set MPC (CCS-MPC). Considering the finite set of possible switching states of the power converters, FCS-MPC select the switching state that minimizes the cost function. And similar to DTC, FCS-MPC directly outputs the switching state to the inverter, usually causes large current and torque ripples and variable switching frequency operation. In CCS-MPC, cost function selection is same as FCS-MPC. But, the output is a continuous voltage vector which can be applied to the inverter through a PWM modulator. CCS-MPC can decrease the current and torque ripples and can achieve the same dynamic performance as FCS-MPC. MPC techniques for PMSM drives have been proposed in [1], [5].

A Model Predictive Control – Space Vector Modulation (MPC-SVM) technique for PMSM drives is proposed in this paper, combines the advantage of both SVM technique and MPC, which overcomes the problem of large torque and flux ripples and it provides a fixed switching frequency for the voltage source inverter that feeds the motor which gives good steady state and dynamic performances.

## II. MATHEMATICAL MODEL OF PMSM

To analyze multiphase machines, the two phase equivalent circuit model is a perfect solution. The mathematical model of PMSM can be done in rotating d-q reference frame.

The d-q axis voltage equations of PMSM are

$$v_d = R_s i_d + \frac{d\varphi_d}{dt} - \varphi_q \frac{d\theta}{dt} \quad (1)$$

$$v_q = R_s i_q + \frac{d\varphi_q}{dt} + \varphi_d \frac{d\theta}{dt} \quad (2)$$

Where  $v_d$  and  $v_q$  are d-axis and q-axis stator voltages,  $i_d$  and  $i_q$  are d-axis and q-axis stator currents,  $\varphi_d$  and  $\varphi_q$  are d-axis and q-axis flux linkages,  $R_s$  is the stator resistance and  $\theta$  is the rotor angle.

The d-axis and q-axis flux linkages are usually defined as

$$\varphi_d = L_d i_d + \varphi_f \quad (3)$$

$$\varphi_q = L_q i_q \quad (4)$$

Where  $L_d$  and  $L_q$  are d-axis and q-axis synchronous inductances,  $\varphi_f$  is the permanent magnet flux. The electrical model in (1) and (2) can be rewritten as (5) and (6).

$$v_d = R_s i_d + L_d \frac{di_d}{dt} - \omega_s L_q i_q \quad (5)$$

$$v_q = R_s i_q + L_q \frac{di_q}{dt} + \omega_s L_d i_d + \omega_s \varphi_f \quad (6)$$

Where  $\omega_s$  is the rotor electrical speed. The mechanical equation of the model can be derived as

$$T_e = T_l + J \frac{d\omega_r}{dt} + B \omega_r \quad (7)$$

Where  $T_e$  is the electromagnetic torque,  $T_l$  is the load torque,  $\omega_r$  is the rotor mechanical speed,  $J$  is the moment of inertia and  $B$  is the shaft friction coefficient. The expression for electromagnetic torque is

$$T_e = \frac{3}{4} p (\varphi_d i_q + \varphi_q i_d) \quad (8)$$

By substituting (3) and (4) to (8),  $T_e$  can be expressed as

$$T_e = \frac{3}{4} p (\varphi_f i_q + (L_d - L_q) i_q i_d) \quad (9)$$

The electromagnetic torque consists of two parts, the permanent magnet torque and the reluctance torque. For a surface mounted PMSM, d and q axis inductance are equal to the synchronous inductance. The torque does not include the reluctance torque and can be simplified as:

$$T_e = \frac{3}{4} p (\varphi_f i_q) \quad (10)$$

### III. MPC-SVM CONTROL OF PMSM

The block diagram of MPC-SVM fed PMSM drive system is shown in Fig. 1. The actual speed is compared with the reference speed and is given to the PI controller to get the torque reference. Stator flux reference can be obtained according to MTPA (Maximum Torque per Ampere) principle. These two references are fed to the MPC controller. The voltage vector that minimizes the difference between reference value and predicted value is selected and it is generated by the inverter through SVM.

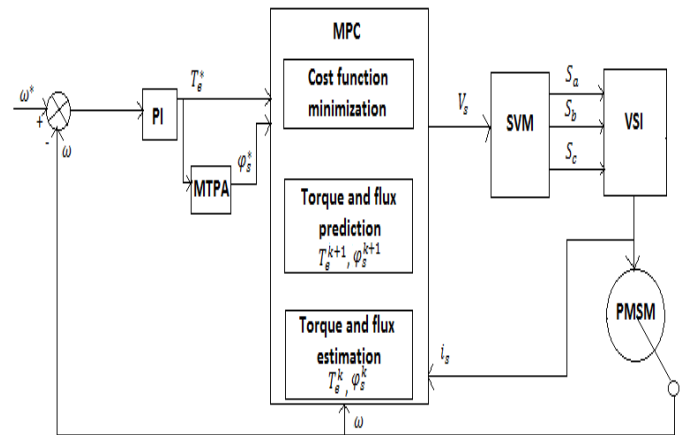


Fig. 1: MPC-SVM fed PMSM drive system

#### A. MPC of PMSM

The cost function of MPC can be defined in such a way that both the torque and stator flux, which is the greatest concern of PMSM drive applications, should be as close as possible to the reference values at the end of the control period. The cost function  $G$  can be defined as

$$\min. G = |T_e^* - T_e^{k+1}| + k_1 |\varphi_s^* - \varphi_s^{k+1}| \quad (11)$$

Where  $T_e^*$  and  $\varphi_s^*$  are the reference values of torque and flux,  $T_e^{k+1}$  and  $\varphi_s^{k+1}$  are the predicted values of torque and flux. In order to unify these terms, a weighting factor  $k_1$  is introduced.

From (5) and (6), the stator currents in d-q reference frame can be expressed as

$$\frac{di_d}{dt} = \frac{-R_s i_d + \omega_s L_q i_q + v_d}{L_d} \quad (12)$$

$$\frac{di_q}{dt} = \frac{-R_s i_q - \omega_s L_d i_d + v_q - \omega_s \varphi_f}{L_q} \quad (13)$$

By using Euler formula, the prediction equation of stator currents (d-q) at instant  $k + 1$  can be obtained as

$$i_d^{k+1} = i_d^k + \frac{1}{L_d} (-R_s i_d^k + \omega_s^k L_q i_q^k + v_d^k) T_s \quad (14)$$

$$i_q^{k+1} = i_q^k + \frac{1}{L_q} (-R_s i_q^k - \omega_s^k L_d i_d^k + v_q^k - \omega_s^k \varphi_f) T_s \quad (15)$$

Where  $v_d^k$ ,  $v_q^k$ ,  $i_d^k$ ,  $i_q^k$ ,  $\omega_s^k$  are the stator voltages, stator currents and rotor electrical speed at instant  $k$ .  $T_s$  is the sampling time. With the knowledge of future stator current, both electromagnetic torque and d-q flux linkages at instant  $k + 1$  can be calculated as

$$\varphi_d^{k+1} = L_d i_d^{k+1} + \varphi_f \quad (16)$$

$$\varphi_q^{k+1} = L_q i_q^{k+1} \quad (17)$$

$$T_s^{k+1} = \frac{3}{4} p(\varphi_d^{k+1} i_q^{k+1} + \varphi_q^{k+1} i_d^{k+1}) \quad (18)$$

To eliminate one step delay in digital implementation, the cost function in (11) should be changed to (19).

$$\min. G = |T_s^* - T_s^{k+2}| + k_1 |\varphi_s^* - \varphi_s^{k+2}| \quad (19)$$

Where  $T_s^{k+2}$  and  $\varphi_s^{k+2}$  are the electromagnetic torque and stator flux at instant  $k + 2$ . To obtain this, a two step prediction is required.

### B. Voltage Space Vector Modulation

The SVM is a special scheme which is used to generate the voltages that can be applied to the stator phases and it comes from the translation of a voltage reference vector in to an amount of time of commutation for each power switches. The voltage vectors generated by a three phase inverter divide the space vector plane into six sectors as shown in Fig. 2.

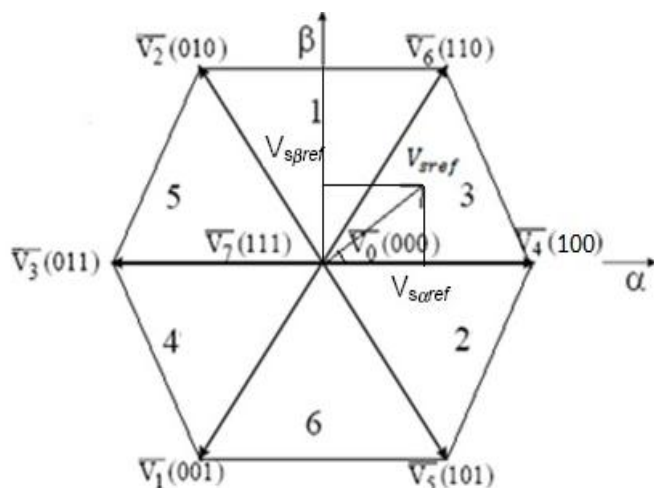


Fig. 2: Space vector diagram

Consider that the reference voltage vector  $V_{sref}$  is in the third sector. The application time of each adjacent vector is given in (20) and reference voltage vector can be expressed as in (21).

$$T = T_4 + T_6 + T_0 \quad (20)$$

$$V_{sref} = \frac{T_4}{T} V_4 + \frac{T_6}{T} V_6 \quad (21)$$

Where T is the total time period and the work times of voltage vectors  $V_4, V_6, V_0$  are  $T_4, T_6$  and  $T_0$ . The amount of times of application of each adjacent vector can be calculated as

$$T_4 = \frac{T}{2V_{dc}} (3V_{saref} - \sqrt{3} V_{s\beta ref}) \quad (22)$$

$$T_6 = \sqrt{3} \frac{T}{V_{dc}} V_{s\beta ref} \quad (23)$$

Where  $V_{dc}$  is the rectified DC voltage and  $V_{saref}, V_{s\beta ref}$  are the  $\alpha$ - $\beta$  components of the reference voltage. Rest of the period is spent in applying the null vector. There are three variables that are associated with the amount of times of vector application and is given as

$$X = \sqrt{3} \frac{T}{V_{dc}} V_{s\beta ref} \quad (24)$$

$$Y = \sqrt{3} \frac{T}{2V_{dc}} V_{s\beta ref} + 3 \frac{T}{2V_{dc}} V_{saref} \quad (25)$$

$$Z = \sqrt{3} \frac{T}{2V_{dc}} V_{s\beta ref} - 3 \frac{T}{2V_{dc}} V_{saref} \quad (26)$$

For sector 3,  $T_4 = -Z$  and  $T_6 = X$ . There is a need of knowledge of the sector in which the voltage vector defined by  $V_{saref}, V_{s\beta ref}$  is found. Generally, the application durations of the sector boundary vectors can be tabulated as shown in Table 1.

Table 1: Durations of the sector boundary vectors

SECTOR	1	2	3	4	5	6
$T_1$	Z	Y	-Z	-X	X	-Y
$T_2$	Y	-X	X	Z	-Y	-Z

The three duty cycles can be computed as

$$t_{aon} = \frac{T - T_4 - T_6}{2} \quad (27)$$

$$t_{bon} = t_{aon} + T_4 \quad (28)$$

$$t_{con} = t_{bon} + T_6 \quad (29)$$

The Table 2 depicts assigning of the right duty cycle to the right motor phase according to the sector.

Table 2: Assigned duty cycles

SECTOR	1	2	3	4	5	6
PHASE						
$S_a$	$t_{bon}$	$t_{aon}$	$t_{aon}$	$t_{con}$	$t_{bon}$	$t_{con}$
$S_b$	$t_{aon}$	$t_{con}$	$t_{bon}$	$t_{bon}$	$t_{con}$	$t_{aon}$
$S_c$	$t_{con}$	$t_{bon}$	$t_{con}$	$t_{aon}$	$t_{aon}$	$t_{bon}$

### IV. SIMULATION OF THE PROPOSED SYSTEM

The proposed MPC-SVM fed PMSM drive system is modeled in MATLAB/Simulink. The sampling frequency is set to 20kHz. The overall simulation diagram is shown in Fig. 3.

In the Simulink model, a three phase voltage source of 415V amplitude and 50 hz frequency is applied to a three phase voltage source inverter with IGBT switches through a diode bridge and is fed to the PMSM motor, which is modelled in d-q reference frame as shown in Fig. 4 and Fig. 5. The motor parameters used for simulation is shown in Table 3. The capacitance of the dc link capacitor across the inverter is set to 1  $\mu$ F. The reference speed of 100rad/s is

compared with the actual motor speed and is given to the PI controller to generate  $T_s^*$  and  $\varphi_s^*$  is determined based on the principle of maximum torque per ampere in order to improve system efficiency.

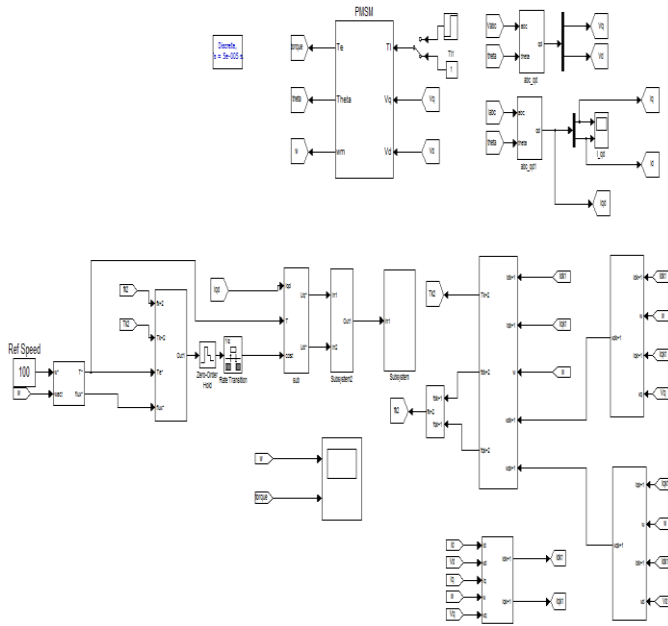


Fig. 3: Simulink model of ,MPC-SVM fed PMSM drive System

Table 3: Motor parameters

Pole number, $p$	6
Permanent magnet flux, $\varphi_f$	.1057Wb
Sator resistance, $R_s$	1.8ohm
d-axis and q-axis inductance, $L_d, L_q$	1.5mH
DC bus voltage, $V_{dc}$	200V

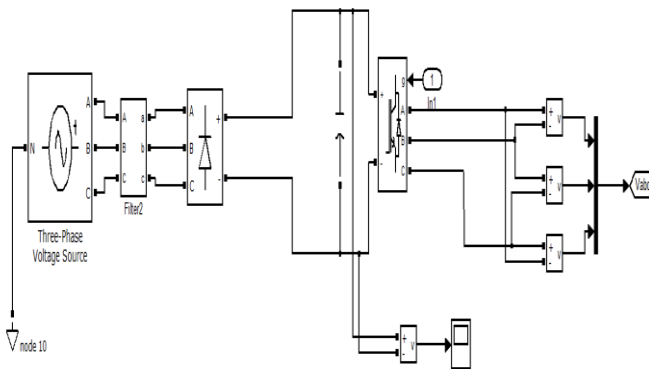


Fig. 4: Simulink model of three phase voltage source fed VSI

For surface PMSM, the relationship between  $T_s^*$  and  $\varphi_s^*$  is

$$|\varphi_s^*| = \sqrt{\varphi_f^2 + \left(\frac{L_q T_s^*}{\frac{3}{2} P \varphi_f}\right)^2} \tag{30}$$

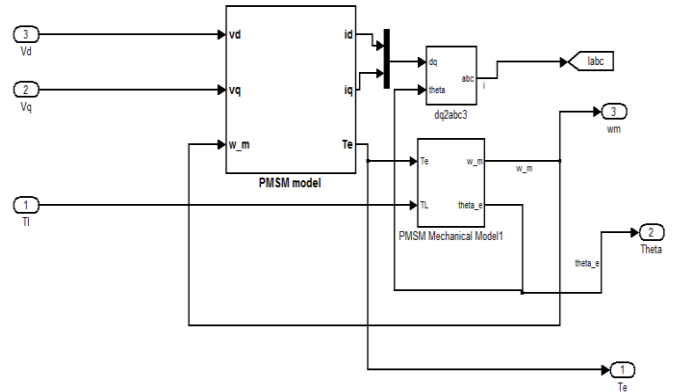


Fig. 5: Simulink model of PMSM

The three phase voltages  $V_a, V_b$  and  $V_c$  are converted in to two phase voltages  $v_d, v_q$  by Park transformation. The mechanical load torque  $T_l$  can be given as a constant value or step value. The two phase currents  $i_d, i_q$ , electromagnetic torque  $T_e$ , rotor speed and position are obtained using (5), (6), (7) and (9). The two phase currents  $i_d, i_q$  are converted in to three phase output currents by using inverse Park transformation.

In Fig. 6, the prediction of current has been done by using (14), (15). To predict the voltages, replace  $i_d, i_q$  by  $i_d^{k+1}, i_q^{k+1}$  in (5), (6) and the modelling is shown in Fig. 7. A two step prediction is preferred in this system to eliminate one step delay in digital implementation. In Fig. 8, current is again predicted by replacing  $i_d^{k+1}, i_q^{k+1}$  by  $i_d^{k+2}, i_q^{k+2}$ , d-q axis currents at instant  $k + 2$  and  $i_d^k, i_q^k$  by  $i_d^{k+1}, i_q^{k+1}$  in (14), (15). Flux and torque predictions can be done by using (16), (17), (18). Finally, the cost function optimization function are obtained by using (19) as shown in Fig. 9. The weighting factor  $k_1$  is set to 25.4.

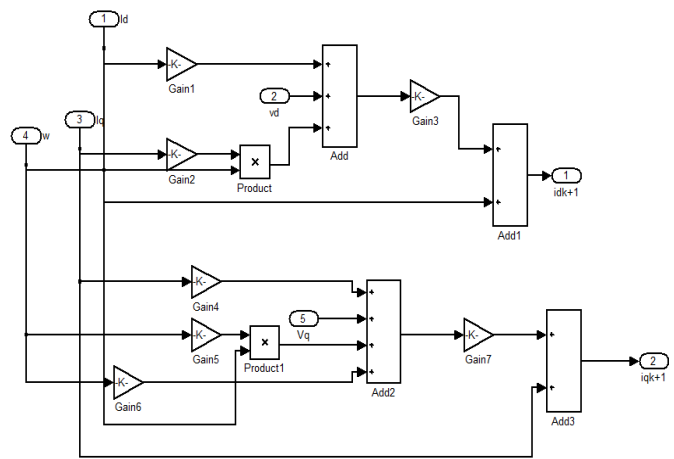


Fig. 6: Simulink model of prediction of current

Fig. 10 shows the SVM generation and the switching frequency is set to 1kHz. The voltages in d-q reference frame that can be obtained and they are converted in to  $\alpha$ - $\beta$  reference frame by Clark transformation. Sector N is calculated. Commutation durations are calculated by using (24), (25), (26). The calculation of application duration of two sector boundary vectors can be done according to the

Table 1 and necessary duty cycles are computed by using (27), (28), (29) for the proper switching of inverter switches.

The three phase line to line output voltages, stator currents, electromagnetic torque and speed waveforms are shown in Fig. 11, Fig. 12 and Fig. 13 with the application of constant load torque. When a step change in load torque is given at 0.6sec, speed decreases to 96rad/sec as shown in Fig. 14.

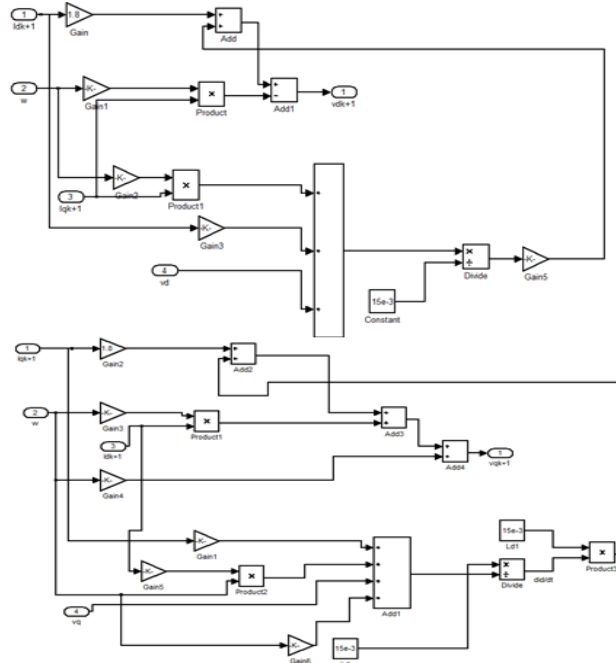


Fig. 7: Simulink model of prediction of d and q axis voltages

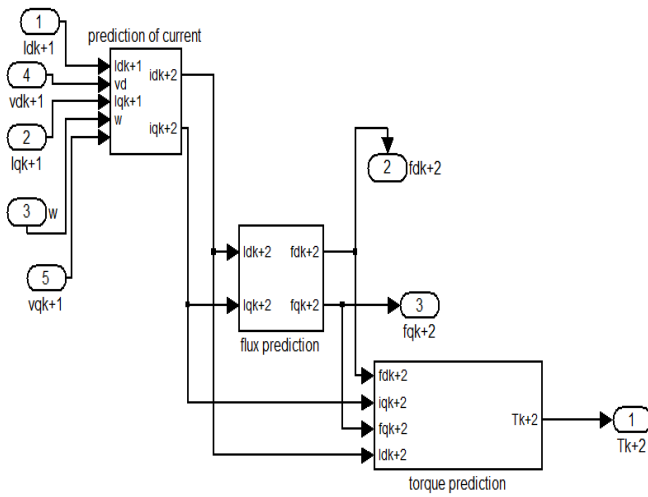


Fig. 8: Simulink model of flux and torque prediction

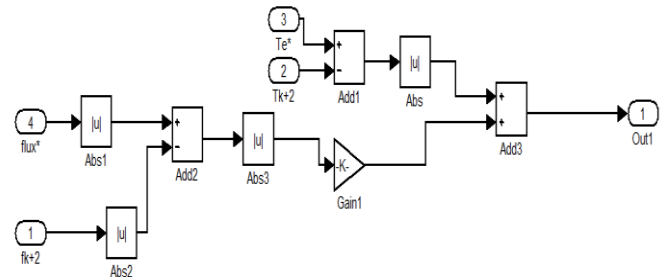


Fig. 9: Simulink model of cost function optimization

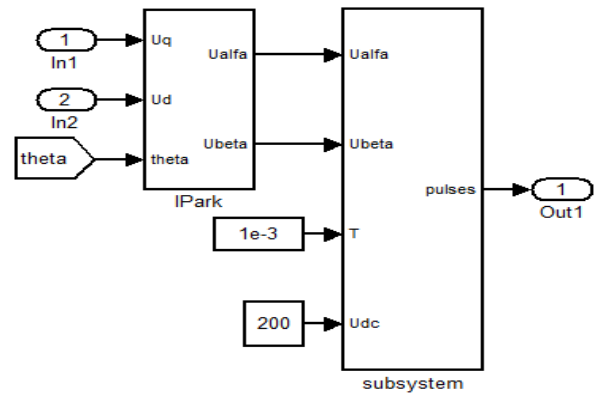


Fig. 10: Simulink model of SVM generation system

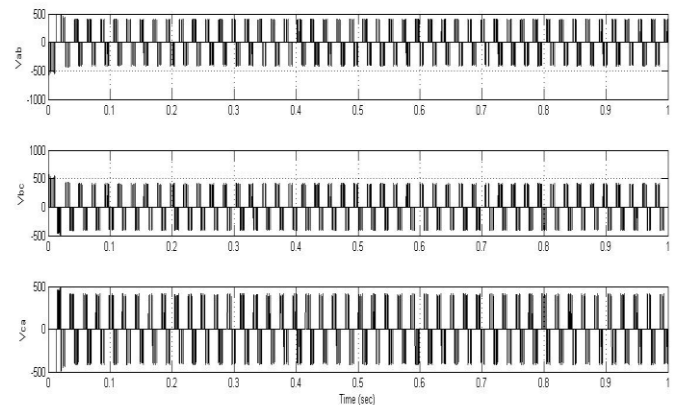


Fig. 11: Simulated waveforms of three phase line to line voltages of PMSM

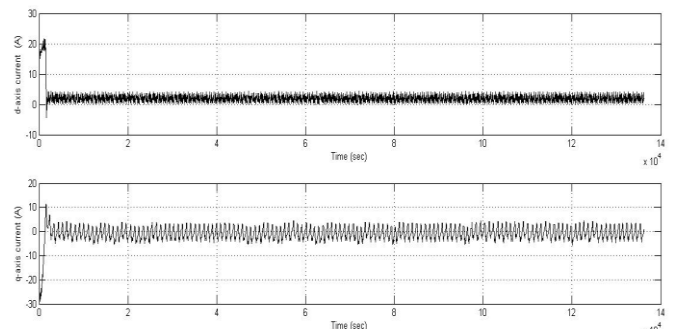


Fig. 12: Simulated waveforms of two axis currents of PMSM



## V. CONCLUSION

In this work, the MPC of PMSM with SVM technique is successfully modelled and simulated in MATLAB/SIMULINK. For designing controllers, MPC is a very powerful concept and its great flexibility of the cost function is the most attractive feature. The advantages of using SVM control strategy is that, it is having high utilization of DC voltage, easy to digital implementation, provides constant switching frequency operation and reduce torque and flux linkage pulsations, which gives fast and good dynamic response.

Simulation results are analyzed by the output waveforms and it shows that the proposed system is having less flux linkage and torque ripples and maintains a good torque and speed response.

## REFERENCES

- [1] Zhixun Ma, Saeid Saeidi and Ralph Kennel, "FPGA implementation of Model Predictive Control with constants switching frequency for PMSM drives", IEEE transactions on industrial informatics, Volume. 10, No. 5, November 2014.
- [2] C. French and P. Acarnley, "Direct Torque Control of permanent magnet drives", IEEE transactions on industrial applications, Volume. 32, 1996.
- [3] C. Lascu and A. M. Trzynadlowski, "Combining the principles of Sliding Mode, Direct Torque Control, and Space Vector Modulation in a high performance sensoreless AC drive", International conference on industrial applications, Volume. 3, 2002.
- [4] Tianshi Wang, Jianguo Zhu, Yongchang Zhang, "Model Predictive Torque Control for PMSM with duty ratio optimization", International conference on electrical machines and systems, August 2011.
- [5] Y. Yang and J. Zhu, "Predictive torque control of permanent magnet synchronous motor drive with reduced switching frequency", International conference on electrical machines and systems, 2010.
- [6] S. Belkacem, B. Zegueb and F. Naceri, "Robust non linear direct torque and flux control of adjustable speed sensorless PMSM drive based on SVM using a PI predictive controller", Journal of engineering science and technology, July 2008.

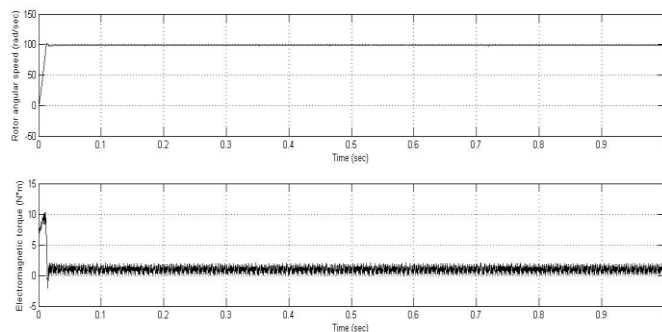


Fig. 13: Simulated waveforms of rotor angular speed and electromagnetic torque of PMSM with constant load torque

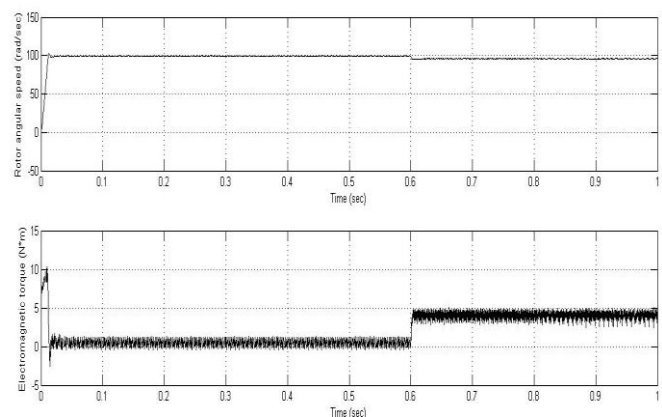


Fig. 14: Simulated waveforms of rotor angular speed and electromagnetic torque of PMSM with a step change in load torque